IOP Publishing Plasma Physics and Controlled Fusion
Plasma Phys. Control. Fusion **62** (2020) 014010 (8pp) https://doi.org/10.1088/1361-6587/ab45c5

# High-quality 5 GeV electron bunches with resonant multi-pulse ionization injection

**P Tomassini[2], D Terzani, F Baffigi, F Brandi, L Fulgentini, P Koester, L Labate[1], D Palla and L A Gizzi[1]**

Intense Laser Irradiation Laboratory, INO-CNR, Pisa, Italy

E-mail: paolo.tomassini@ino.it

Received 24 July 2019, revised 4 September 2019
Accepted for publication 18 September 2019
Published 24 October 2019

**Abstract**

The production of high-quality electron bunches in laser wakefield acceleration relies on the possibility of injecting ultra-low emittance bunches in the plasma wave. A new bunch injection scheme (resonant multi-pulse ionization, ReMPI) has been conceived and studied, in which electrons extracted by ionization are trapped by a large-amplitude plasma wave driven by a train of resonant ultrashort pulses. Such a train of pulses can be obtained in a very efficient, compact and stable way, by phase manipulation in the laser front-end. The ReMPI injection scheme relies on currently available laser technology and is being considered for the implementation of future compact x-ray free electron laser schemes. Simulations show that high-quality electron bunches with an energy of up to 5 GeV and a peak current exceeding 2 kA, with normalized emittance of below 0.1 mm $\times$ mrad and a slice energy spread of below 0.1%, can be obtained with a single stage.

Keywords: laser-plasma acceleration, high-brightness beams, resonant multi-pulse ionization injection, multi-pulse laser wake field acceleration, free electron lasers, high-quality electron beams

(Some figures may appear in colour only in the online journal)

## 1. Introduction

Laser wakefield accelerators (LWFA) are nowadays approaching the 10 GeV energy scale [1], with accelerating gradients in the order of 40 GeV $m^{-1}$. Several applications of those electron bunches, including staging [2–6], LWFA-based colliders [7–9] and high-quality secondary sources [10–16] can now be envisaged. Therefore, a viable laser wakefield accelerator producing GeV scale, high-quality, electron bunches should operate with a flexible and stable injection mechanism capable of producing very low emittance bunches.

Several electron injection schemes have been proposed and tested so far. Among them, ionization injection [17–25] opens up the possibility of experimental control of the injection mechanism. Injection via density downramp [26–30] has been proven to be capable of generating very low emittance bunches [28], though it is not easy to disentangle the mean energy, the energy spread, the charge and the emittance of the produced bunch.

The need for a flexible scheme capable of generating very low emittance bunches led to the introduction of the two-color ionization injection [31]. The two-color ionization scheme needs the use of two laser systems. The 'driver' pulse excites the plasma wave and is delivered by a long-wavelength (e.g $CO_2$) system, while a synchronised pulse (the 'ionization' pulse) from a Ti:Sa system extracts the electrons from the dopant by tunnel field-ionization. To date, however, long-wavelength ($\lambda > 5\ \mu$m), high-power ($P > 100$ TW) and ultrashort ($T \ll 100$ fs) laser systems are lacking and hopefully will be available in the near future.

The new resonant multi-pulse ionization injection scheme (ReMPI) [32] is capable of generating very low emittance bunches in a flexible way, yet using a single Ti:Sa laser system. In ReMPI, the long-wavelength driver pulse of the two-color injection is substituted by a train of pulses that excites the wakefield through the multi-pulse LWFA

[1] Also at INFN, Sect. of Pisa, (Italy).
[2] Author to whom any correspondence should be addressed.

 

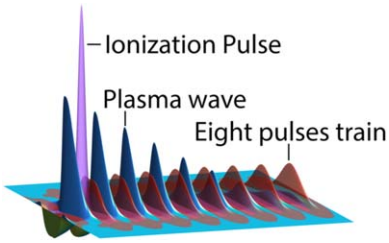


**Figure 1.** The ReMPI scheme. The incoming pulse passes through a beam splitter; a portion is time shaped as a train of eight pulses (red, transparent surface), while a smaller portion in fourth harmonics is tightly focused in the rear of the train (purple surface) and extracts electrons from the argon dopant. The driver train resonantly excites a high-amplitude plasma wave (black line) that traps and accelerate the electrons.

mechanism [33–36], maintaining each pulse's electric field under the ionization threshold for the selected dopant (e.g. nitrogen or argon). Subsequently, a tightly focused, low amplitude, pulse in second, third or fourth harmonics in the tail of the train ionizes the dopant, thus injecting the electrons into the wakefield with an ultra-low emittance (see figure 1). While the ReMPI scheme has been already (numerically) tested for producing low-charge ($Q \simeq 5$pC) high-quality beams [32, 37, 38], relatively high-charge ($Q \simeq 30$ pC) high-quality explorations of the scheme were still lacking.

In this paper we report on numerical simulations about the trapping and acceleration of a 5 GeV electron bunch, with a beam-quality high enough to drive a free electron laser (FEL), as envisaged in the EuPRAXIA project [39]. FELs are extremely demanding in terms of beam quality [40, 41], especially at their high energy end, where radiation with wavelength $\lambda_R \simeq \lambda_U/2\gamma^2 \approx 1\,\mathring{A}$ (here $\lambda_U \approx 2$ cm is the undulator period) can be generated. In addition to standard beam-quality parameters, the so-called 'slice quality' parameters should be evaluated for a bunch aiming at driving a FEL. Slice parameters refer to the phase space quality of each transverse slice of the bunch, and give us relevant information on which slice will participate in FEL lasing. In the case of the EuPRAXIA envisioned FEL, the required global and slice parameters at the undulator entrance are summarized in the 'requested' row of table 1.

The working configuration shown here is based on a 1PW Ti:Sa laser system, temporally shaped into a train of eight pulses in the fundamental harmonics, each delivering 6.3J in 55 fs. Moreover, a 45 fs long pulse in the fourth harmonics, obtained by an amplified portion of the same master pulse of the train, is tightly focused behind the driver, thus constituting the ionization pulse. The experimental arrangement can deal either with multiplexing techniques after the amplification chain [34–36, 42] or with the new TEMPI scheme, recently proposed by Labate *et al* and tested with start-to-end simulations [43, 44]. TEMPI is based upon the usage of birefringent plates of increasing thicknesses and crossed polarizations, which produce delayed replicas of the original pulse, and linear polarizers [45]. In contrast to the arrangement described in [45], in TEMPI such a stack is used, on the stretched pulse, early in the CPA amplification chain, thus allowing for a recovering of the pulse energy at a relatively small price in terms of additional pump energy. The TEMPI scheme should result in a more compact and stable setup with respect to the above mentioned schemes, yet be able to generate a train of pulses with almost constant peak intensity along the train and with an energy conversion efficiency approaching unity. Finally, we stress that being the driving train and the ionization pulse amplified replicas of the same master pulse, no synchronization jitter issues are raised. Nonetheless, $\mu$m sized mechanical vibrations can induce some fluctuations in the ionization pulse-to-driver train delay, but those fluctuations can be safely maintained at (some) femtoseconds level, i.e. to a very small fraction of the plasma period. The laser train and ionization pulse parameters have been collected in table 2.

The plasma target consists of a two adjacent sections stack. In the first section, made by a gas-cell filled with a mixture of argon (50%) and helium, electrons are extracted by field ionization and subsequently trapped by the plasma wave. Finally, electrons experience a longitudinal phase-rotation that reduces their overall energy spread to a percent level. In this first section the laser pulse is still focusing, therefore a guiding parabolic channel is not necessary here. The second section is placed as close as possible to the cell and consists of a gas capillary filled by pure helium. In the capillary the laser pulse remains focused and can excite the plasma wave for about 25 cm [1]. In both stages, background plasma density is set to $n_e = 2.1 \times 10^{17}\,\mathrm{cm}^{-3}$, which sustains a plasma wave of wavelength 75 $\mu$m.

Simulations of about 25 cm of propagation in the plasma have been performed with the hybrid fluid/PIC code QFluid [46]. The QFluid simulations assume a 2D *cylindrical* symmetry of the fields, while particles of the bunch move in a full 3D space. The bunch is sampled with $N_b \approx 10^6$ equal-weighted macroparticles and the simulation box (a cylinder, actually) has radius 320$\mu$m and length 690 $\mu$m. QFluid is equipped with a mesh-refining technique, which is activated in the longitudinal portion of the cylinder where the bunch is placed. The fields are solved by quasi-static approximation [47] by using the coarse resolution of $dz_{\mathrm{coarse}} = 0.47\mu$m (longitudinal) and $dr_{\mathrm{coarse}} = 0.93\,\mu$m (radial), while the refined grid spacing are $dz_{\mathrm{fine}} = 0.012\,5\,\mu$m and $dr_{\mathrm{fine}} = 0.1\,\mu$m.

We remark that the evolution of the laser pulse's complex envelope [48] has been performed maintaining the second order derivative in the time evolution, thus ensuring the most accurate description of the (very long) pulse's evolution.

## 2. Driving pulse train evolution

The evolution of the driver train as a whole is highly non-trivial, due to propagation of the pulses in a nonuniform plasma. A detailed analysis of this evolution is beyond the scope of the present work and will be presented elsewere [49]. However, as the first pulse propagates in a steady, uniform plasma, it starts exciting the wakefield, which is reinforced by the subsequent pulses via a resonant process. We point out

**Table 1.** Requested beam quality ('R' raw) and quality parameters obtained by means of the simulations reported in the paper ('O' raw). The overall and slice relative energy spread $\sigma(E)/E$ and normalised emittance $\epsilon_n$, as well as the total charge $Q$ and peak current $I$, are shown.

| Param. | $\sigma(E)/E$ | $\epsilon_n$ | $\sigma(E)/E\|_{slice}$ | $\epsilon_n\|_{slice}$ | $Q$ | $I$ |
|---|---|---|---|---|---|---|
| R | $<1$, % | $\ll 1$ $\mu$mrad | $<0.1\%$ | $\ll 1$ $\mu$mrad | $\geqslant 30$ pC | $>1$ kA |
| O | 0.9% | 0.085 $\mu$mrad | 0.03% (min) | 0.085 $\mu$mrad | 30 pC | 2.5 kA |

**Table 2.** Relevant parameters set for the driving train and the ionization pulse. The total delivered energy ($E$), the FWHM pulse(s) duration ($T$), the minumum waist ($w_0$), the pulse-to-pulse delay (the ionization pulse refers to the last pulse of the train) and the normalized pulse amplitude ($a_0$) are shown.

| Laser | E | T | $w_0$ | Delay | $a_0$ |
|---|---|---|---|---|---|
| Driver | 50 J | 55 fs | 90 $\mu$m | 250 fs | 0.63 |
| Ionization | 0.06 J | 45 fs | 5.9 $\mu$m | 85 fs | 0.25 |

that in such a framework, all the driver pulses behind the first one interact with a perturbed plasma density which can strongly affect their evolution. Therefore, different portions of a given driver pulse, depending on its length and phase in the plasma wave, could be refracted away or focused. Moreover, the energy exchange from the pulse and the wave can vary significantly from the usual scenario.

In the simulation shown here, some optimization procedure has been employed to stabilize the evolution of the pulses in the tail of the driving train. Nevertheless, a sizable fluctuation of the peak intensity is still present during the 25 cm of propagation, as is shown in figure 2(a). The severe pump depletion of about 70% of laser energy is mostly due to erosion of the last pulses in the train, as is now apparent in figure 2(b), while not only the first pulse shows a depletion of just a 10 % (not shown there) but also experiences a strong self-focusing. Nonetheless, the train is capable of exciting a large-amplitude plasma wave for most of its propagation distance, as will be shown in the next section.

## 3. Tunnel field-ionization of bunch electrons

In the first target section containing argon, it is supposed that the laser prepulse and the first few cycles of the first driver pulse are able to ionize the gas up to the eighth level. This is because the ionization energies of the first eight electrons are relatively low, with the highest being about 144 eV. In the passage to the K-shell (i.e. to the ninth electron), however, a large jump in the ionization energy occurs ($U_{i,9} \simeq 422$ eV), thus realizing the optimal conditions for a controlled extraction of the electrons with an ad hoc large-amplitude electric field. This is accomplished by focusing the fourth harmonic 'ionization' pulse behind the train, in such a way that its electric field is close to its threshold for the $Ar^{8+} \rightarrow Ar^{9+}$ transition. It is worth noting that the electric field amplitude of a laser pulse is proportional to its normalized amplitude $a_0 = eA_0/mc^2$ and to its wavevector $k_0 = 2\pi/\lambda_0$, $\lambda_0$ and $a_0$ being the pulse wavelength and vector potential amplitude, respectively. Therefore, a large electric field amplitude can be realized with a moderate normalized amplitude $a_0$ but with a very short wavelenght. If a Ti:Sa pulse is chosen ($\lambda \simeq 800$ nm), a fourth harmonics conversion is an efficient, yet cumbersome, option. In the following, a fourth harmonics converted pulse will be considered, along with the resulting normalized amplitude $a_{0,ion} = 0.25$ and a minimum waist of $w_{0,ion} = 5.8$ $\mu$m.

Once the electron leaves the atom, it starts to quiver in the oscillating pulse electric and magnetic fields and, after the ionizing pulse has overpassed it, a residual secular transverse momentum along the polarization axis is left, thus constituting a source of bunch emittance. Analytical results and simulations in [50], show that the minimum normalized emittance achievable by using a linearly polarized pulse can be as low as

$$\epsilon_{n,\min} \simeq \frac{1}{\sqrt{2}} w_{0,ion} \cdot a_{0,ion} \cdot \Delta^2 = \frac{1}{\sqrt{2}} w_{0,ion} \cdot a_{0,ion}^2/a_c, \quad (1)$$

with $\Delta \equiv \sqrt{a_{0,ion}/a_c}$, $a_c = 0.108 \cdot \lambda_{ion}(U_i/U_H)^{3/2}$ ($U_H \simeq 13.6$ eV; see equation (26) in [50] and (4) in [32]). Having selected the transition $Ar^{8+} \rightarrow Ar^{9+}$, along with the above mentioned ionizing pulse, we derive from equation (1) a minimum achievable 'thermal' emittance of $\epsilon_{n,\min} \simeq 0.05$ $\mu$mrad. We mention, however, that other mechanisms can be responsible for an emittance increase. Though the ponderomotive forces are a good linear approximation in the transverse coordinate and consequently do not contribute to the transverse emittance (see [50]), the transverse kick on the low-energy electrons increases the beam radius just after the pulse passage and causes a fraction of the beam lying in a region of nonlinear transverse force. Those electrons, therefore, will oscillate with a lower betatron frequency, thus partially spoiling out the transverse quality. Moreover, as bunch charge increases, space charge and beam loading can contribute to increasing the beam emittance. In our simulations a final emittance of $\epsilon_{nx} = 0.08$ $\mu$mrad in the first section has been obtained, which should be compared with the minimum value of 0.05 $\mu$mrad obtained with equation (1).

## 4. Bunch trapping and energy boosting up to 5 GeV

Once the newborn electrons are extracted by the ionizing pulse, they slip back in the wake while they are accelerated by the electric field. Those electrons are trapped by the wave, provided that they reach the wake (phase) velocity prior to entering into its decelerating region. The trapping, therefore, occurs if the wake accelerating field exceeds some threshold

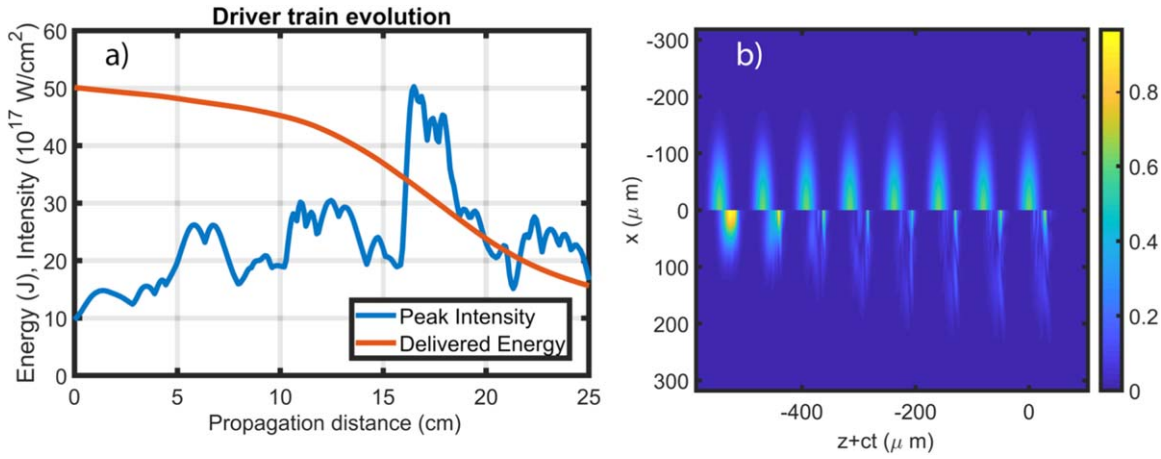


**Figure 2.** Driver train evolution. (a) Peak intensity and overall pulse energy evolution. (b) Initial (upper) and final (lower) maps of the pulse envelope. Pulses move towards the left.

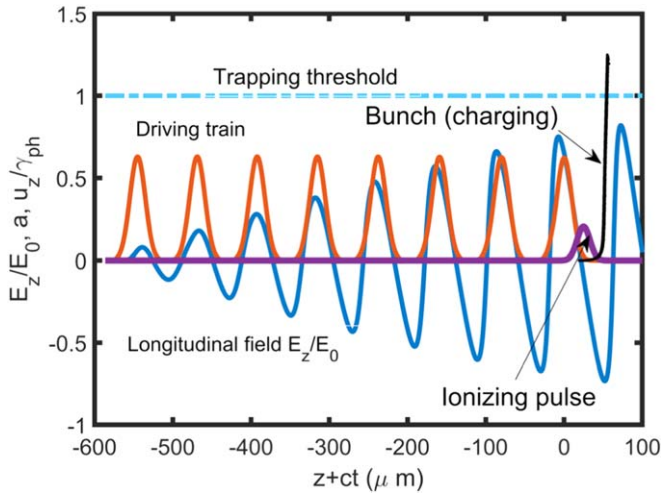


**Figure 3.** An axis snapshot at the early stage of bunch trapping. Lineout of the driving train (red line) and of the ionizing pulse (purple line) normalized amplitudes, as well as the lineout of the longitudinal normalized electric field $E_z/E_0$ are shown. The Lorentz factor $\gamma$ associated with the wakefield is $\gamma_{ph} \simeq 90$. The longitudinal phase space of the bunch (black dots) is $(z + ct\,[\mu m],\, u_z/\gamma_{ph})$, where $u_z = -p_z/mc$. Particles with $u_z/\gamma_{ph} \geqslant 1$ are trapped by the wave.

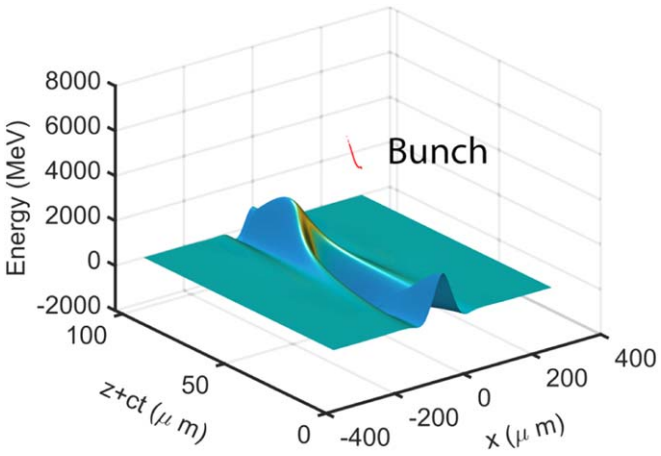


**Figure 4.** The phase-space $((z + ct)[\mu\text{m}],\, x[\mu\text{m}],\, E[\text{MeV}])$ of the bunch at the end of the 25 cm (aprrox.) long capillary. The longitudinal electric field map is also shown.

that depends on the exact phase of the wake where the the electrons are frozen. In our simulations electrons reach the wake's speed well before its node, which means that trapping occurs within the standard trapping and the 'strong' trapping [32] condition boundaries. In figure 3 a snapshot of the bunch longitudinal phase-space is shown, at a time in which electrons are still being extracted from the dopant. The bunch (black dots) is already partially trapped, while most of the particles still have a longitudinal momentum $u_z = -p_z/mc$ well below the trapping threshold $\gamma_{ph} = 1\Big/\sqrt{1 - \beta_{ph}^2} \simeq 90$, $\beta_{ph} = v_{ph}/c$ being the phase speed of the wake. In figure 3 the driving pulse train (red line) and ionization pulse (purple line) are also shown. After the last train pulse, a nonlinear wave (blue line) with amplitude $E_z/E_0 \simeq 0.7$ has been excited (here $E_0 = mc\,\omega_p/e$ is the nonrelativistic wavebreaking limit and $\omega_p$ is the plasma frequency). As the bunch is fully trapped by the wave, a longitudinal phase-space rotation occurs. Moreover, transverse focusing forces remain linear inside the bunch, which is adiabatically squeezed down to a (quasi round) beam of about 0.8 $\mu$m diameter.

After the phase-space rotation, the train and the bunch enter into the helium-filled capillary, which guides the laser for more than 20 cm. Notwithstanding the nontrivial evolution of the laser pulses (as shown in section 2), the bunch always experiences linear focusing forces, though the accelerating fields varies considerably during the propagation. Yet, a mean accelerating gradient of $\simeq$45 GV m$^{-1}$ has been obtained, which corresponds to a mean normalized field $E_z/E_0 \simeq 0.45$. At the end of the capillary, the driving train is depleted by its 70% and the bunch energy is about 5 GeV, with a marginal increase of the normalized emittance up to $\epsilon_{nx} = 0.085$ $\mu$mrad and $\epsilon_{ny} = 0.080$ $\mu$mrad. The final beam phase-space, along with the longitudinal electric field in its bucket, are shown in figure 4.

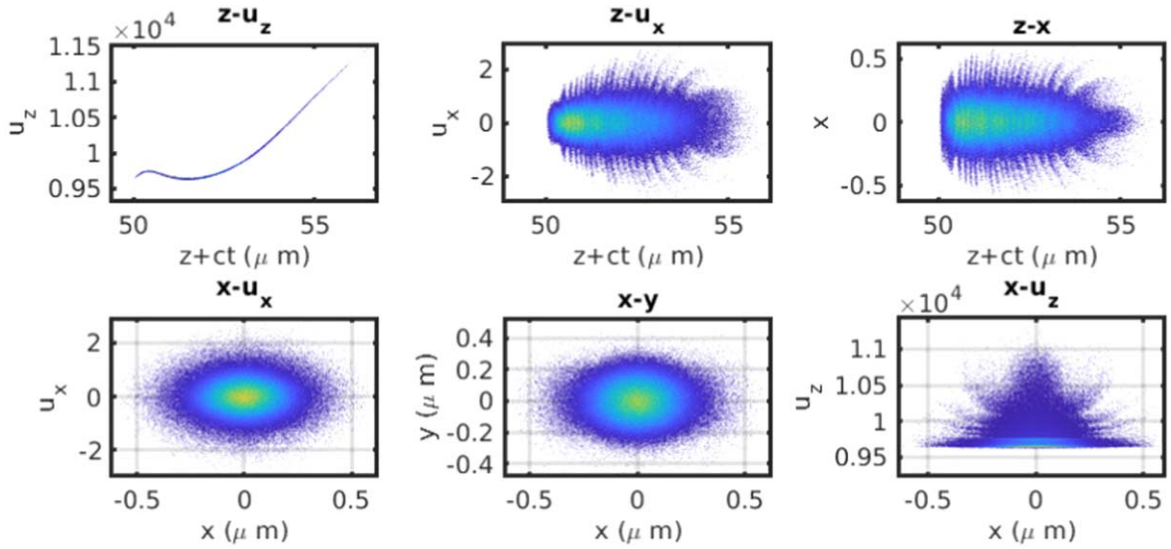


**Figure 5.** Phase-space cuts of the final beam. Here $u_{x,y} = p_{x,y}/mc$ and $u_z = -p_z/mc$. The bunch moves towards the left.

## 5. Final bunch quality

As we pointed out in the introduction, a FEL oriented beam should be analyzed in both the overall and slice perspectives. While the projected (overall) one gives us relevant information about quality degradation during the beam transport lines [51, 52], a slice inspection of the phase space will definitely show us which (and how) portions of the bunch will participate in lasing [40, 41]. In figure 5 some cuts of the 6D final phase space are shown. As is apparent from cuts in the $x - y$ and $x - u_x$ planes, a (quasi) round and matched beam has been obtained. The $z - u_z$ plane, however, shows us that a higher energy tail is present. This tail partially spoils the longitudinal beam quality, the overall energy spread being about 1.8%. A better inspection of the longitudinal phase-space cut, however, reveals that only a small fraction of the beam charge (about 8%, actually) is responsible for the high-energy tail and of the subsequent large energy spread (see figure 6). The tail is therefore easily removed with a simple tuning of the transfer line energy acceptance. The transported beam (with about 92% of the total charge, i.e 30 pC) complies with all the (projected) requirements of the 'requested' raw in table 1, its overall energy spread being $\sigma_E/E = 0.9\%$.

Slice analysis of the bunch phase space has been performed with a slice thickness of 0.1 $\mu$m, which is compatible with the cooperation length of the envisioned FEL setup [40]. In figure 7(a) the slice current profile, as well as brightness-5D ($B_{5D} \equiv 2I/(\pi^2 \epsilon_{nx} \times \epsilon_{ny})$) and brightness-6D ($B_{6D} \equiv B_{5D}/(\sigma_E/E/10^3)$) are shown. Remarkably, at least brilliance-5D is about a factor of three above the one recently obtained with a two-stage LWFA/PWFA hybrid approach (see [53], where a definition of brightness without the $\pi$'s has been used). Moreover, the current distribution shows a gentle-varying profile with peak value of 3.7 kA. In figure 7(b) the normalized emittances along the $x$ (ionization) and $y$ (driver) polarization axis are reported. At peak current, i.e at a longitudinal position of about $-1$ $\mu$m from the bunch center-of-mass, emittances of 0.065 $\mu$mrad and 0.04 $\mu$mrad along the $x$- and $y$-axis are reported. Remarkably, the slice energy spread reported in figure 7(c) shows an excellent distribution, with more than 80% of the bunch charge in slices having an energy spread of less than the required upper limit of 0.1%. Finally the minimum slice energy spread is attributed to a slice in the head of the bunch and in position $-1.4$ $\mu$m. That slice possesses the highest brightness, having extremely low emittances of 0.045 $\mu$mrad and 0.03 $\mu$mrad, an energy spread of 0.03% and a current 2 kA.

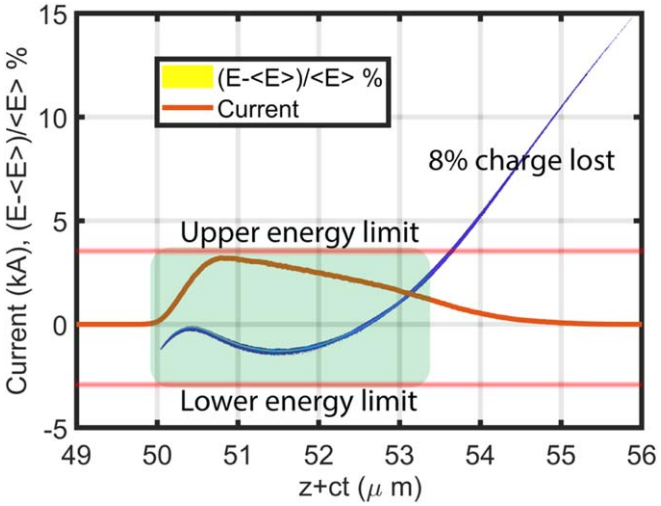


**Figure 6.** Longitudinal phase-space plot ($(z + ct)[\mu\text{m}]$, $(E - <E>)/<E>$) and current profile of the final beam. By selecting a standard beam optics with maximum energy below $1.3 \times <E>$, about 92% of the bunch charge is transported to the final undulator stage for lasing.

## 6. Sensitivity to parameter fluctuations

Several laser and plasma parameters can affect the final beam quality. Fluctuations on the delivered laser pulse energy, for example, is directly linked to variation on both the

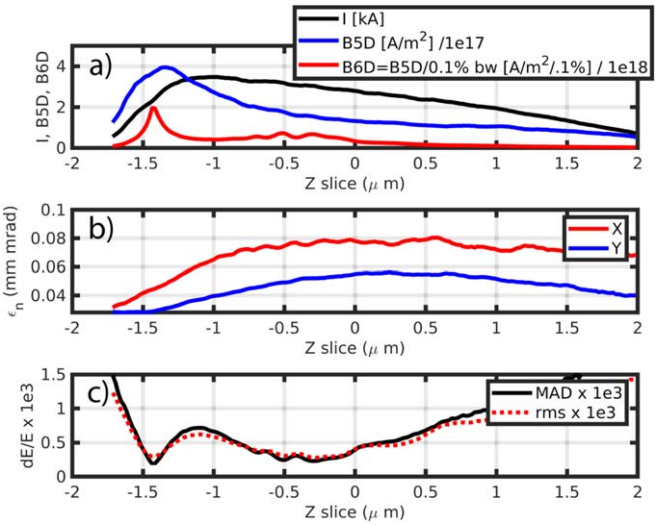


**Figure 7.** Slice analysis with slice thickness 0.1 $\mu$m The longitudinal axis corresponds to the slice position with respect to beam center-of-mass. (a) Current (black), brightness-5D $B_{5D} \equiv 2I/(\pi^2\epsilon_{nx} \times \epsilon_{ny})$ (blue) and brightness-6D $B_{6D} \equiv B_{5D}/(\sigma_E/E/10^3)$ (red). (b) Emittances in the $x$ (red) and $y$ (blue) directions. (c) Energy spread using the *rms* estimator (red, dashed) and the mean absolute deviation robust indicator (black).

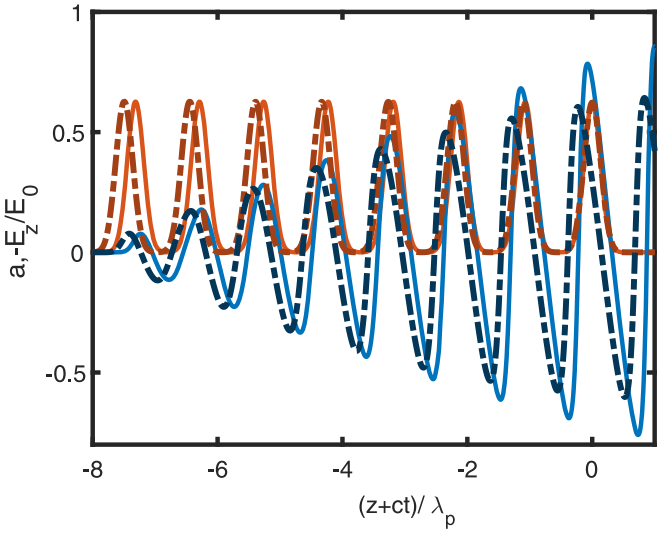


**Figure 8.** Sensitivity of the accelerating field (blue lines) on the resonance condition mismatch. The horizontal axis refers to the number of plasma periods and in the vertical axis both the accelerating field and pulses amplitude (orange) are shown. While in the optimized case (full lines) the peak accelerating field reaches the value of $E_{z,ref} = 0.7E_0$, the wakefield excited in a plasma with a background density increased by 5% (dashed lines) has peak value $E_z = 0.55E_0$, showing a reduction of more than 20%.

accelerating field amplitude and phase (due to nonlinear plasma wavelengh increase), while variations in the background density mostly affect the resonance condition for the wave excitation. A full evaluation of the final beam parameters' stability against most of the working point parameters has been performed for a setup related to a 150 MeV injector for the EuPRAXIA 5 GeV line [54], where a background density of about $1 \cdot 10^{18}\,\mathrm{cm}^{-3}$ was used. There, we found that the selected working point is stable, provided that 'reasonable' conditions for the upper limit of the experimental conditions fluctuations were satisfied. As an example, a 1% level of maximum admissible delivered pulse energy should be assured so as to limit the mean final energy fluctuation to about 1%. Pulse-to-pulse delay $T_D$ (timing) jitter can be responsible of a resonance condition loss, therefore inducing a fluctuation in the wakefield amplitude (and phase) unless $N\delta(\omega_p \cdot T_D)/(\omega_{p,ref} \cdot T_{D,ref}) \ll 1$, where $N = 8$ is the number of pulses of the train and the subscript *ref* refers to the reference value of the parameter. Therefore, the experimental scheme that generates a time modulation in the laser pulse must possess a very good stability ($\delta T_D/T_{D,ref} \ll 1/N$). The TEMPI scheme, which was selected for the experimental demonstration of the ReMPI, shows a virtually null pulse-to-pulse jitter: the replicas of the stretched pulse (about 1 ps long) are produced by a mechanically stable stack of birefringent crystals and polarizers and overlap until they leave the compressor. We also mention that the time jitter between the pulse train and the ionizing pulse possesses potential detrimental effects on beam quality. However, being both the driving train and the ionization pulses amplified replicas of the same master pulse, the time jitter between them is only due to mechanical vibrations and can be safely limited to a few $\mu$m, which should be compared with the plasma wavelength $\lambda_p \simeq 75$ $\mu$m. Plasma density fluctuations result in the most severe source of beam-quality fluctuations. The resonance condition refers to the plasma period, which depends on the local background density $n_0 = n_{0,ref} + \delta n_0$. Since the efficient resonant excitation of the wave can be rewritten as $\delta n_0/n_{0,ref}/2 + \delta T_D/T_{D,ref} \ll 1/N$, extremely low (of percent size) background density fluctuations can be acceptable. This can be made clearer by figure 8, where the pulse train and its excited wakefield is shown in two different cases: the optimized case with the couple of parameters ($T_{D,ref}$, $n_{0,ref}$) (full lines) and a case with the couple ($T_{D,ref}$, $n_{0,ref} + \delta n_0$), being $\delta n_0 = 5\%\ n_{0,ref}$ (or, alternately, the couple ($T_{D,ref} + 2.5\%\ T_{D,ref}$, $n_{0,ref}$), shown with the dashed lines). From figure 8 we can infer that a variation of 5% of the plasma density, or equivalently, a variation of about 2.5% of the time delay of all the pulses, will cause cause a reduction of more than 20% in the wakefield amplitude, thus reinforcing the claim that the background plasma density must be controlled at about one percent level.

## 7. Conclusions

We have shown, by means of hybrid fluid/PIC simulation, that a FEL-quality 5 GeV electron bunch can be obtained with a single-stage LWFA. In order to employ the ReMPI injection scheme, the 1PW Ti:Sa laser system is equipped with a longitudinal pulse-shaper that modulates the pulse envelope in a sequence of eight pulses which drive a large amplitude plasma wave. Just after the pulse train, a low-intensity fourth harmonic converted portion of the initial pulse is tightly focused, so as to act as an 'ionization pulse'. The argon

K-shell electrons are extracted by tunnel ionization in the ionizing pulse field and are subsequently trapped by the wakefield. Finally, after about 25 cm of propagation in a capillary filled with helium, they are accelerated up to the desired energy of 5 GeV. The pulse train evolution is highly nontrivial and will be further investigated in a future work. Despite this, a 30 pC electron bunch with an energy spread of below 1% can be obtained after a standard selection of the beam transport energy range. The normalized emittance, being below 0.1 $\mu$mrad, is about on order of magnitude below the one usually obtained at those energies. Moreover, slice analysis reveals an excellent quality of a large fraction of the slices, with about 80% of the charge in slices having an energy spread below the threshold of 0.1%. We finally mention that a record brilliance-5D of $4 \times 10^{17}$ $A$ $m^{-2}$, along with outstanding properties of the best slice of $\sigma_E/E = 0.03\%$, $\epsilon_{nx} = 0.045$ $\mu$mrad, $\epsilon_{ny} = 0.03$ $\mu$mrad and current of 2 kA, can be obtained. The experimental demonstration of the scheme should face mechanical stabilization at (some of) $\mu$m size of the laser system, the pulse beamline and the interaction area, as usual in high energy LWFA experiments. Moreover, an additional constraint of stable control of the plasma background density at the 1% level is necessary, so as to assure an efficient resonant excitation of the plasma wave.

## Acknowledgments

The research leading to these results has received funding from the EU Horizon 2020 Research and Innovation Program under Grant Agreement No. 653782 EuPRAXIA. This project has received financial support from the CNR funded Italian research Network ELI-Italy.

## ORCID iDs

P Tomassini https://orcid.org/0000-0002-8106-8917

## References

[1] Gonsalves A J *et al* 2019 Petawatt laser guiding and electron beam acceleration to 8 GeV in a laser-heated capillary discharge waveguide *Phys. Rev. Lett.* **122** 084801
[2] Dopp A, Guillaume E, Thaurya C, Lifschitz A, Ta Phuoc K and Malka V 2015 Energy boost in laser wakefield accelerators using sharp density transitions *Phys. Plasmas* **23** 056702
[3] Steinke S *et al* 2016 Staging of laser-plasma accelerators *Phys. Plasmas* **23** 056705
[4] Audet T L *et al* 2016 Electron injector for compact staged high energy accelerator *Nucl. Instrum. Methods Phys. Res.* A **829** 304–8
[5] Golovin G, Banerjee S, Chen S, Powers N, Liu C, Yan W, Zhang J, Zhang P, Zhao B and Umstadter D 2016 Control and optimization of a staged laser-wake field accelerator *Nucl. Instrum. Methods Phys. Res.* A **830** 375–80
[6] Zhang Z *et al* 2016 Energy spread minimization in a cascaded laser wakefield accelerator via velocity bunching *Phys. Plasmas* **23** 053106
[7] Schroeder C B, Esarey E, Geddes C G R, Toth C and Leemans W P 2009 *Advanced Accelerator Concepts* (vol 1086) ed C B Schroeder, E Esarey and W Leemans (New York: AIP) pp 208–14
[8] Schroeder C B, Esarey E, Geddes C G R, Benedetti C and Leemans W P 2010 Physics considerations for laser-plasma linear colliders *Phys. Rev. Spec. Top. Accel. Beams* **13** 101301
[9] Muggli P and Cros B 2018 ALEGRO, the advanced linear collider study group *IX International Particle Accelerator Conf. IPAC* (https://accelconf.web.cern.ch/AccelConf/ipac2018/papers/tupml036.pdf)
[10] Nakajima K 2008 Few femtosecond, few kiloampere electron bunch produced by a laser–plasma accelerator *Nat. Phys.* **4** 92–3
[11] Petrillo V *et al* 2013 Observation of time-domain modulation of free-electron-laser pulses by multipeaked electron-energy spectrum *Phys. Rev. Lett.* **111** 114802
[12] Loulergue A, Labat M, Evain C, Benabderrahmane C, Malka V and Couprie M E 2015 Beam manipulation for compact laser wakefield accelerator based free-electron lasers *New J. Phys.* **17** 023028
[13] Esarey E, Ride S K and Sprangle P 1993 Nonlinear Thomson scattering of intense laser pulses from beams and plasmas *Phys. Rev.* E **48** 3003
[14] Tomassini P, Giulietti A, Giulietti D and Gizzi L A 2005 Thomson backscattering x-rays from ultra-relativistic electron bunches and temporally shaped laser pulses *Appl. Phys.* B **80** 419–36
[15] Corde S, Ta Phuoc K, Lambert G, Fitour R, Malka V, Rousse A, Beck A and Lefebvre E 2013 Femtosecond x rays from laser-plasma accelerators *Rev. Mod. Phys.* **85** 1
[16] Micieli D, Drebot I, Bacci A, Milotti E, Petrillo V, Rossetti Conti M, Rossi A R, Tassi E and Serafini L 2016 Compton sources for the observation of elastic photon-photon scattering events *Phys. Rev. Spec. Top. Accel. Beam.* **19** 093401
[17] Chen M, Sheng Z-M, Ma Y-Y and Zhang J 2006 Electron injection and trapping in a laser wakefield by field ionization to high-charge states of gases *J. Appl. Phys.* **99** 056109
[18] Pak A, Marsh K A, Martins S F, Lu W, Mori W B and Joshi C 2010 Injection and trapping of tunnel-ionized electrons into laser-produced wakes *Phys. Rev. Lett.* **104** 025003
[19] McGuffey C *et al* 2010 Ionization induced trapping in a laser wakefield accelerator *Phys. Rev. Lett.* **104** 025004
[20] Thaury C *et al* 2015 Shock assisted ionization injection in laser-plasma accelerators *Sci. Rep.* **5** 16310
[21] Clayton C E *et al* 2010 Self-guided laser wakefield acceleration beyond 1 GeV using ionization-induced injection *Phys. Rev. Lett.* **105** 105003
[22] Chen M, Esarey E, Schroeder C B, Geddes C G R and Leemans W P 2012 Theory of ionization-induced trapping in laser-plasma accelerators *Phys. Plasmas* **19** 033101
[23] Zeng M, Chen M, Yu L L, Mori W B, Sheng Z M, Hidding B, Jaroszynski D A and Zhang J 2015 Multichromatic narrow-energy-spread electron bunches from laser-wakefield acceleration with dual-color lasers *Phys. Rev. Lett.* **114** 084801
[24] Zeng M, Luo J, Chen M, Mori W B, Sheng Z-M and Hidding B 2016 High quality electron beam acceleration by ionization injection in laser wakefields with mid-infrared dual-color lasers *Phys. Plasmas* **23** 063113
[25] Audet T L *et al* 2016 Investigation of ionization-induced electron injection in a wakefield driven by laser inside a gas cell *Phys. Plasmas* **23** 023110

[26] Bulanov S, Naumova N, Pegoraro F and Sakai J 1998 Particle injection into the wave acceleration phase due to nonlinear wake wave breaking *Phys. Rev.* E **58** R5257
[27] Suk H, Barov N, Rosenzweig J B and Esarey E 2001 Plasma electron trapping and acceleration in a plasma wake field using a density transition *Phys. Rev. Lett.* **86** 1011–4
[28] Tomassini P, Galimberti M, Giulietti A, Giulietti D, Gizzi L A, Labate L and Pegoraro F 2003 Production of high-quality electron beams in numerical experiments of laser wakefield acceleration with longitudinal wave breaking *Phys. Rev. Spec. Top. Accel. Beams* **6** 121301
[29] Geddes C G R, Cormier-Michel E, Esarey E, Nakamura K, Plateau G R, Schroeder C B, Toth C, Bruhwiler D L, Cary J R and Leemans W P 2008 Plasma gradient controlled injection and postacceleration of high quality electron bunches *Proc. of the Thirteenth Advanced Accelerator Concepts Workshop* 1086
[30] Buck A *et al* 2013 Shock-front injector for high-quality laser-plasma acceleration *Phys. Rev. Lett.* **110** 185006
[31] Yu L-L, Esarey E, Schroeder C B, Vay J-L, Benedetti C, Geddes C G R, Chen M and Leemans W P 2014 Two-color laser-ionization injection *Phys. Rev. Lett.* **112** 125001
[32] Tomassini P, De Nicola S, Labate L, Londrillo P, Fedele R, Terzani D and Gizzi L A 2017 The resonant multi-pulse ionization injection *Phys. Plasmas* **24** 103120
[33] Umstadter D, Esarey E and Kim J 1994 Nonlinear plasma waves resonantly driven by optimized laser pulse trains *Phys. Rev. Lett.* **72** 1224
[34] Hooker S M, Bartolini R, Mangles S P D, Tunnermann A, Corner L, Limpert J, Seryi A and Walczak R 2014 Multi-pulse laser wakefield acceleration: a new route to efficient, high-repetition-rate plasma accelerators and high flux radiation sources *J. Phys.* B **47** 234003
[35] Shalloo R J, Corner L, Arran C, Cowley J, Cheung G, Thornton C, Walczak R and Hooker S M 2016 Generation of laser pulse trains for tests of multi-pulse laser wakefield acceleration *Nucl. Instrum. Methods Phys. Res.* A **829** 383–5
[36] Cowley J *et al* 2017 Excitation and control of plasma wakefields by multiple laser pulse *Phys. Rev. Lett.* **119** 044802
[37] Tomassini P, Labate L, Londrillo P, Fedele R, Terzani D and Gizzi L A 2017 High-quality electron bunch production for high-brilliance Thomson Scattering sources *Proc. vol 10240, Laser Acceleration of Electrons, Protons, and Ions IV*102400T (https://doi.org/10.1117/12.2266938)
[38] Tomassini P, De Nicola S, Labate L, Londrillo P, Fedele R, Terzani D, Nguyen F, Vantaggiato G and Gizzi L A 2018 High-quality GeV-scale electron bunches with the resonant multi-pulse ionization injection *Nucl. Inst. Meth. Phys. Res.* A **909** 1–4
[39] Walker P A *et al* 2017 Horizon 2020 EuPRAXIA design study *J. Phys.: Conf. Series* **874** 012029
[40] Dattoli G, Ottaviani P L and Pagnutti S Booklet for FEL Design (http://fel.enea.it/booklet/pdf/Booklet_for_FEL_design.pdf)
[41] Dattoli G, Renieri A and Torre A 1993 *Lectures on Free Electron Laser Theory and Related Topics* (Singapore: World Scientific)
[42] Siders C W, Siders J L W, Taylor A J, Park S-G and Weiner A M 1998 *Appl. Opt.* **37** 5302–5
[43] Toci G, Mazzotta Z, Labate L, Mathieu F, Vannini M, Patrizi B and Gizzi L A 2019 Conceptual design of a laser driver for a plasma accelerator user facility *Instruments* **3** 40
[44] Labate L *et al* Efficient pulse train generation in Ti:Sa CPA systems in preparation
[45] Dromey B, Zepf M, Landreman M, Okeeffe K, Robinson T and Hooker S M 2007 Generation of a train of ultrashort pulses from a compact birefringent crystal array *Appl. Opt.* **46** 5142–6
[46] Tomassini P and Rossi A R 2016 Matching strategies for a plasma booster *Plasma Phys. Control. Fusion* **58** 034001
[47] Sprangle P, Esarey E and Ting A 1990 Nonlinear theory of intense laser-plasma interaction *Phys. Rev. Lett* **64** 2011–4
[48] Sprangle P, Esarey E and Krall J 1996 Self-guiding and stability of intense optical beams in gases undergoing ionization *Phys. Rev.* E **54** 4211
[49] Tomassini P *et al* Evolution of pulse trains in long-range propagation MP-LWFA in preparation
[50] Schroeder C B, Vay J-L, Esarey E, Bulanov S, Benedetti C, Yu L-L, Chen M, Geddes C G R and Leemans W P 2014 Thermal emittance from ionization-induced trapping in plasma accelerators *Phys. Rev. Spec. Top. Accel. Beams* **17** 101301
[51] Migliorati M, Bacci A, Benedetti C, Chiadroni E, Ferrario M, Mostacci A, Palumbo L, Rossi A R, Serafini L and Antici P 2013 Intrinsic normalized emittance growth in laser-driven electron accelerators *Phys. Rev. Spec. Top. Accel. Beams* **16** 011302
[52] Li X, Chancé A and Nghiem P A P 2019 Preserving emittance by matching out and matching in plasma wakefield acceleration stage *Phys. Rev. Accel. Beams* **22** 021304
[53] Martinez de la Ossa A *et al* 2019 Hybrid LWFA PWFA staging as a beam energy and brightness transformer: conceptual design and simulations *Phil. Trans. Royal Soc.* A **377** 20180175
[54] Tomassini P, Terzani D, Labate L, Toci G, Chance A, Nghiem P A P and Gizzi L A 2019 High quality electron bunches for a multi-stage GeV accelerator with the Resonant Multi-Pulse Ionization injection *Phys. Rev. Accel. Beams* submitted for publication